

Maternal metabolic stress may affect oviduct gatekeeper function

L. Jordaens^a, V. Van Hoeck^a, V. Maillo^b, A. Gutierrez-Adan^b, W. Marei^{a,c}, B. Vlaeminck^d, S. Thys^e, R. Sturmeij^f, P.E.J. Bols^a, J.L.M.R. Leroy^a

^a *Laboratory for Veterinary Physiology and Biochemistry, Gamete Research Center, University of Antwerp, Universiteitsplein 1, B-2610 Wilrijk, Belgium*

^b *INIA, Instituto Nacional de Investigacion y Tecnologia Agraria y Alimentaria, Carretera de La Coruna, 28040 Madrid, Spain*

^c *Department of Theriogenology, Faculty of Veterinary Medicine, Cairo University, Giza 12211, Egypt*

^d *Laboratory for Animal Nutrition and Animal Product Quality, Ghent University, Belgium*

^e *Laboratory for Cell Biology and Histology, Core Facility for Biomedical Microscopic Imaging, University of Antwerp, Groenenborgerlaan 171, B-2020 Antwerp, Belgium*

^f *Hull York Medical School, Center for Cardiovascular and Metabolic Research, University of Hull, Cottingham Road, Hull HU6 7RX, United Kingdom*

¹Corresponding author: Lies Jordaens; Laboratory for Veterinary Physiology and Biochemistry, Gamete Research Centre, University of Antwerp, Universiteitsplein 1, B-2610 Wilrijk, Belgium; +32 3 265 23 98; lies.jordaens@uantwerpen.be

Short title: NEFAs and oviduct physiology

Abstract

We hypothesized that elevated non-esterified fatty acids (NEFA) modify *in vitro* bovine oviduct epithelial cell (BOEC)-metabolism and barrier function. Hereto, BOECs were studied in a polarized system with 24h-treatments at day 9: 1) CONTROL (0 μ M NEFA + 0%EtOH), 2) SOLVENT CONTROL (0 μ M NEFA + 0.45%EtOH), 3) BASAL NEFA (720 μ M NEFA + 0.45%EtOH in the basal compartment), 4) APICAL NEFA (720 μ M NEFA + 0.45%EtOH in the apical compartment). FITC-albumin was used for monolayer permeability assessment, and related to Transepithelial Electric Resistance (TER). Fatty acid (FA), glucose, lactate and pyruvate concentrations were measured in spent medium. Intracellular lipid droplets (LD) and **FA-uptake** were studied using Bodipy 493/503 and **immunolabelling of FA-transporters (FAT/CD36, FABP3 and CAV1)**. BOEC-mRNA was retrieved for qRT-PCR. Results revealed that APICAL NEFA reduced relative TER-increase (46.85%) during treatment, and increased FITC-albumin flux (27.59%) compared to other treatments. In BASAL NEFA, FAs were transferred to the apical compartment as free FAs: mostly palmitic and oleic acid increased, respectively 56.0 % and 33.5% of initial FA-concentrations. APICAL NEFA allowed no FA-transfer, but induced LD-accumulation **and upregulated FA-transporter expression (\uparrow CD36, \uparrow FABP3, \uparrow CAV1)**. Gene expression in APICAL NEFA indicated increased anti-apoptotic (\uparrow *BCL2*) and anti-oxidative (\uparrow *SOD1*) capacity, upregulated lipid metabolism (\uparrow *CPT1*, \uparrow *ACSL1* and \downarrow *ACACA*), **and FA-uptake (\uparrow CAV1)**. All treatments had similar carbohydrate metabolism and oviduct function specific gene expression (=OVGP1, ESR1, FOXJ1). Overall, elevated NEFAs affected BOEC-metabolism and barrier function differently depending on NEFA-exposure side. Data substantiate the concept of the oviduct as a gatekeeper that may actively alter early embryonic developmental conditions.

Key word: NEFAs, oviduct, TER, fatty acid transfer, metabolism

Introduction

In dairy cattle, extensive genetic selection to promote milk yield has led to a drastic increase in energetic demands and reduced fertility (Leroy *et al.* 2008a, Leroy *et al.* 2008b). To support increased milk production, dairy cow metabolism shifts to prioritize lactation, causing metabolic stress, which can be manifested through increased lipolysis and elevated serum concentrations of non-esterified fatty acids (NEFAs) (Leroy *et al.* 2005). Similar observations have been described in women where metabolic stress, associated with e.g. obesity and type II diabetes, is linked with lipolytic disorders (Lash & Armstrong 2009).

Elevated serum NEFAs are reflected in the ovarian follicular fluid (Leroy *et al.* 2004, Leroy *et al.* 2005, Robker *et al.* 2009) and are recognized as important factors affecting fertility. As such, NEFAs have direct detrimental effects on murine folliculogenesis (Valckx *et al.* 2014), bovine oocyte nuclear maturation and developmental capacity (Jorritsma *et al.* 2004, Leroy *et al.* 2005, Aardema *et al.* 2011, Van Hoeck *et al.* 2011) and the quality of the resulting embryo (Van Hoeck *et al.* 2011). In women and mice, oocyte quality has also been related to metabolic alterations in follicular fluid (Valckx *et al.* 2012, Valckx *et al.* 2015) with potentially lasting adverse effects in the offspring (Jungheim *et al.* 2011).

In addition, it has been demonstrated that elevated NEFAs can affect *in vitro* bovine oviduct epithelial cell (BOEC) physiology (Jordaens *et al.* 2015). Elevated NEFAs hampered BOEC physiology by reducing cell proliferation, cell migration capacity, cell functionality and monolayer integrity, in a cell polarity dependent manner. However, insights in the pathways associated to these observations and in cellular responses arising from NEFA-exposure are currently lacking. Furthermore, it's important to learn 'how', 'whether' and 'to which extent' intracellular fatty acid (FA)-uptake and transepithelial transfer of these FAs can occur. Recent *in vivo* experiments indeed indicated that the conditions in the reproductive tract define its ability to sustain early embryo development (Rizos *et al.* 2010, Maillo *et al.* 2012, Matoba *et al.* 2012). As such, the oviductal environment in metabolically stressed lactating dairy cattle was less supportive for blastocyst formation compared to heifers (Rizos

et al. 2010) and to non-lactating cows (Maillo *et al.* 2012). *In vitro* reports suggest this may be due to direct environmental effects of elevated NEFAs, as NEFA-exposure during bovine embryo culture jeopardized embryo quality through reduced blastocyst formation and cell number, with a concomitant rise in apoptosis (Van Hoeck *et al.* 2013) and internalization of FAs (Listenberger *et al.* 2003, Leroy *et al.* 2010). In mice, similar observations have been made as exposure of murine embryos to pathological NEFA-concentrations during *in vitro* culture, induced effects on embryo metabolism and growth (Jungheim *et al.* 2011). However, whether or not elevated serum NEFAs can be transferred across the oviduct epithelial lining and are actually reflected in the oviductal lumen, where they may contribute to suboptimal embryo growth conditions, remains to be elucidated.

It is furthermore unknown whether elevated NEFA concentrations may influence oviduct specific characteristics such as permeability. Earlier Roche *et al.* (2001), reported that FAs altered *in vitro* Caco-2 monolayer confluency by affecting transepithelial electric resistance (TER) and expression of tight junctions. In oviductal cells, a reduced TER and cell migration capacity were observed in the presence of elevated NEFAs (Jordaens *et al.* 2015) but mechanistic insights are currently lacking. Affecting oviduct epithelial permeability and thereby altering the oviduct gatekeeper function would reflect in the overall composition of the oviduct micro-environment as different molecules may be filtered from the serum to the oviductal lumen (Leese *et al.* 2007). NEFAs may therefore also indirectly affect early embryo development.

Studies expanding on the consequences of elevated NEFAs on oviduct cell function and micro-environment are scarce. Possibly, since *in vivo* studies remain challenging to perform due to specialist equipment and techniques, and difficult to interpret considering the complexity of the whole organism (Velazquez *et al.* 2010). Hereto, an *in vitro* polarized cell culture (PCC) system with hanging inserts (Miessen *et al.* 2011; Tahir *et al.*, 2011) may provide a valid alternative, since it promotes preservation of both morphology and biology of native oviduct epithelium (Fotheringham *et al.* 2011) while focusing on immediate cellular responses of oviduct epithelial cells exclusively. It is therefore considered as a valuable tool to acquire primary mechanistic insights in the direct effects of

NEFAs on BOEC physiology. In particular BOEC metabolism and barrier function, oviduct specific functions such as oviduct specific glycoprotein secretion, anti-oxidative and anti-apoptotic characteristics, and cellular FA-transfer or uptake are of interest, as they may influence early embryo development.

Therefore, in the present study, we hypothesized that elevated NEFA-concentrations can affect BOEC physiology by altering BOEC metabolism and barrier function. Hereto, we aimed to obtain a more profound understanding in the direct effects of elevated NEFAs on BOEC physiology and gatekeeper features in a PCC by observing 1) BOEC monolayer integrity and permeability, 2) FA-transfer across the monolayers, 3) intracellular lipid accumulation, 4) BOEC FA-transporters, 5) BOEC energy metabolism, and 6) mRNA expression of genes related to BOEC viability, oxidative stress, BOEC specific functions and both carbohydrate and lipid metabolism. This research may ultimately further elucidate the direct effects of NEFAs on the oviductal micro-environment, affecting pre-implantation embryo development. This may contribute to the complex pathogenesis of infertility associated with lipolytic metabolic disorders.

Materials and Methods

All chemicals were purchased from Thermo Fisher Scientific® (Carlsbad, California, USA), unless stated otherwise.

Primary BOEC-culture: isolation and culture in a polarized cell culture (PCC) system

BOECs were isolated and cultured as described previously (Jordaens *et al.* 2015). Briefly, in each replicate 4 bovine oviducts from cows in the early luteal phase (days 3 to 5 of the estrous cycle) and ipsilateral to the ovulation site were obtained from a local slaughterhouse. As the pre-implantation embryo interacts with both ampulla and isthmus, BOECs from whole oviducts were mechanically isolated within 3h after slaughter. BOEC number and viability were determined, using Trypan Blue exclusion and a hemocytometer, and seeded at a density of 1×10^6 cells/mL in a polarized cell culture (PCC) system with hanging inserts (Corning, Snapwell, 6-well). Each compartment contained 2mL culture medium, based on DMEM/F12 (containing 0.75% w/v BSA (essentially FA free; Sigma-Aldrich,

St-Louis, MO, USA), 5% v/v serum (2.5% v/v Fetal Bovine serum, Greiner Bio-One, Frickenhausen, Germany; and 2.5% v/v Newborn Calf Serum, Sigma-Aldrich, St-Louis, MO, USA), 2.5% v/v penicillin/streptomycin and 2% v/v amphotericin B), and was renewed initially after 24h, subsequently every 48h.

Preparation of the treatments

The types and concentrations of free FAs used are based on the *in vivo* concentrations found in the serum of high yielding dairy cows in negative energy balance (NEB) (Leroy *et al.* 2005). To mimic the FA-profile during NEB, NEFA-concentrations of 720 μ M (i.e. 230 μ M Palmitic Acid (PA) + 280 μ M Stearic Acid (SA) + 210 μ M Oleic Acid (OA)) were implemented as a pathological condition, and prepared as described by Van Hoeck *et al.* (2011). Solubility of lipophilic NEFAs into hydrophilic culture was spectrophotometrically confirmed prior to use.

Experimental design

BOECs were maintained in hanging inserts and supported by medium replenishments of both compartments every 48h until they reached confluency, as confirmed by Transepithelial Electrical Resistance (TER) using an Avometer (Millicell-ERS[®], Millipore, Massachusetts, USA). Monolayer formation was defined confluent when the TER-recordings exceeded 700 Ω .cm² (Chen *et al.* 2015) at Day 9. Ultimately at Day 9 pre-exposure medium samples were collected after which 4 treatments were established: 1) CONTROL: 0 μ M NEFA in both compartments, 2) SOLVENT CONTROL: 0 μ M NEFA + 0.45% v/v EtOH in both compartments, 3) BASAL NEFA: 720 μ M NEFA + 0.45%v/v EtOH in the basal compartment, and 4) APICAL NEFA: 720 μ M NEFA + 0.45% v/v EtOH in the apical compartment. Preparations of NEFA were added to the monolayers at Day 9 for 24h as depicted in figure 1. After 24h (Day 10), outcome parameters were assessed, spent medium from both compartments in all wells was sampled, and BOECs were either collected using EDTA-trypsin for mRNA-extraction or fixed in 4% paraformaldehyde for immunofluorescent staining. Per outcome parameter, samples from a total of 16 animals were used, and analysed as four pools of four.

Outcome parameters:

1. BOEC-integrity and monolayer permeability

TER-measurements were recorded, both prior (Day 9) and post NEFA-exposure (Day 10), to observe monolayer confluence and integrity. Hereto, a Millicell-ERS (Millipore, Massachusetts, USA) was used according to the manufacturer's instructions. Monolayers were considered confluent when TER-values ranged between 700 and 1100 $\Omega\cdot\text{cm}^2$ (Chen *et al.* 2015). Data were expressed as relative TER-increase over the 24h treatment period. At Day 10 and immediately after NEFA-exposure, monolayer permeability was determined by measuring macro-molecular transport of 66kDa FITC-labelled albumin across the monolayers, as described by Chang *et al.* (2013) in endothelial cells with some modifications to suit our design, objective and cell type. Briefly, in 4 repeats (2 inserts per flux direction within each treatment group and per replicate, total number of inserts n= 54) FITC-albumin (15 μM) was dissolved in HBSS without phenol red and added to either the apical or the basal chamber (each 2 wells per treatment per replicate) to observe albumin flux in either direction. Unseeded inserts were used as a positive control to exclude effects due to the membrane properties. After 3h, medium in each compartment was mixed by pipetting and 20 μL samples were submitted for FITC measurement at 490 nm excitation/ 530nm emission using a Tecan microplate reader, Infinite[®] 200 Pro (Tecan Trading AG, Switzerland). Both the supplemented and the non-supplemented compartment were sampled in order to retrospectively correlate the decrease in fluorescence from the supplemented compartment to the increase in fluorescence in the non-supplemented compartment. Standard curves ranged from 0 to 2 μM , however, to match the FITC-albumin concentrations in the supplemented compartment a 10x dilution was required. R²-values of >0.99 and CV<10% were considered valid.

2. BOEC fatty acid transfer capacity

Spent medium from both NEFA-supplemented and their opposite compartments were spectrophotometrically analyzed for total FA-concentrations, gas chromatographically for individual FA-concentrations, and for FA-profiles per FA-fraction (free or esterified) in 4 repeats.

2.1. Total FA-concentrations

Total FA-concentrations were measured at the 'Algemeen Medisch Labo' (AML, Antwerp, Belgium), using commercial photometric assays, RX Daytona (Randox Laboratories) **in 4 replicates with 3 observations per treatment**. Measurements were carried out according to manufacturer's instructions. The intra- and interassay coefficients of variation for all analyses were <5%.

2.2 FA-profiles per FA-fraction (free or esterified)

FAs in spent medium (**in 4 replicates using a pool of 2 inserts per treatment**) were extracted as described by Löfgren *et al.* (2012), with heneicosanoic acid (5 µg) and triheptadecanoin (5 µg) as internal standard. The FA-extract was divided in three aliquots for determination of i) total FAs, ii) FAs in triacylglycerols, cholesteryl-esters and glycerophospholipids (esterified) and iii) non-esterified fatty acids (free).

Total FAs were methylated by a consecutive base-catalyzed and an acid-catalyzed step (Vlaeminck *et al.* 2014). Esterified FAs (in triacylglycerols, cholesteryl-esters and glycerophospholipids) were methylated using only the base-catalyzed step. For separation of the free FAs, the NEFA-containing hexane layer was methylated using an acid catalysed step. Fatty acid methyl esters were subsequently extracted with hexane.

Composition analysis of FA-methyl esters was carried out by gas chromatography (HP7890A, Agilent Technologies, Diegem, Belgium) with a split-splitless injector and flame ionization detector using a SP-2560 column (75m x 0.18 mm i.d. x 0.14 µm thickness, Supelco Analytical, Bellefonte, USA). The carrier gas was hydrogen (flow rate: 1 mL/min) with splitless injection (t° : 50°C for 2.5 min, 175°C for 13 min, and 215°C for 25 min). Inlet and detector temperatures were 250 and 255°C, respectively. Peaks were identified based on retention time comparisons with a mixture of FAME standards (GLC463, Nu-Check-Prep., Inc., Elysian, MN, USA). Quantification of FA-methyl esters was based on the area of the internal standard and on the conversion of peak areas to the weight of FAs by a theoretical response factor for each FA (Ackman & Sipos 1964, Wolff *et al.* 1995).

3. Intracellular lipid accumulation

In three replicates, monolayers from 3 inserts per treatment were fixed at Day 10 of culture (and after NEFA-exposure according to figure 1) in 4% phosphate buffered paraformaldehyde for 10 minutes. BOECs were washed twice with DPBS, and permeabilized with saponin (0.1% w/v) (Carl Roth GmbH&Co, Karlsruhe, Germany). Nuclei were stained with 5 µg/mL DAPI (Molecular Probes, Eugene, OR) for 5 minutes and subsequently washed with DPBS. Neutral lipids were stained with BODIPY 493/503 (Molecular Probes, Ghent, Belgium) (20 µg/mL) in DPBS for 1h, according to a modified protocol of Van Hoeck *et al.* (2013). After staining the insert membranes and monolayers were removed from the insert housing and mounted on a microscope slides with Citifluor (VWR, Haasrode, Belgium). High resolution images were obtained using Nikon Eclipse Ti-E inverted microscope, attached to a microlens-enhanced dual spinning disk confocal system (UltraVIEW VoX; PerkinElmer, Zaventem, Belgium) equipped with 405 and 488nm diode lasers for excitation of blue and green fluorophores, respectively. For each monolayer, 10 random z-stack of 20 µm with each 1 µm intervals, were made starting at the level of the insert membrane. In extended focus images neutral lipid accumulation was compared **qualitatively** among treatments.

4. BOEC fatty acid transporters

At Day 10 of culture (and after NEFA-exposure according to figure 1), 1 BOEC monolayer per treatment was fixed in 4% phosphate buffered paraformaldehyde for 10 minutes in 3 replicates. Monolayers were submitted to immunofluorescent staining, using polyclonal anti-FABP3 rabbit anti-bovine antibodies (MyBiosource), polyclonal anti-CD36 rabbit anti-bovine antibodies (ThermoFisher Scientific), or polyclonal anti-CAV1 rabbit anti-bovine antibodies (Cell Signaling Technology). FITC-conjugated goat anti-rabbit IgG (ThermoFisher Scientific) was used as secondary antibody according to manufacturer's instructions. Protocols were tested for non-specific primary and secondary antibody binding, and bis benzimide (Hoechst no 33342; Sigma-Aldrich) was used as nuclear stain. After staining, the insert membranes and monolayers were removed from the insert housing and mounted on a microscope slides with Citifluor (VWR, California USA). High resolution images were obtained using Nikon Eclipse Ti-E inverted microscope (vide supra '3. Intracellular lipid

accumulation'). For each monolayer, full thickness z-stacks with 0.5 μm intervals, were randomly made to localize the BOEC-FA-transporter expression. To quantify the BOEC FA-transporter expression, 10 random single z-plane images per monolayer were made. Laser settings for the 405nm laser line were used to focus all nuclei in each plane, while 488 nm laser settings were fixed for each transporter type. In each image, total green fluorescence and number of nuclei were measured using Volocity imaging software version 6.3.1 (PerkinElmer, The Netherlands). The level of FA-transporter expression is presented as the mean amount of green fluorescent pixels counted per nucleus.

5. BOEC energy metabolism: glucose, lactate and pyruvate concentrations

Medium sampling was performed pair-wise as repeated measures at Day 9 and Day 10: pre-exposure medium (= routine BOEC, DMEM/F12-based culture medium) was added at Day 8 and sampled at Day 9 after 24h incubation (4 replicates with 3 observations per treatment). Post-exposure medium, containing the different treatments, was subsequently added at Day 9 and sampled 24h later at Day 10. Both pre- and post-exposure medium were prepared from the same batch to assure all composing nutrients were identical. Immediately after collection, all medium samples were centrifuged at 1250 x g (5min, room temperature) to avoid cellular contamination and possible confounding of the results by ongoing cellular activities in the medium. Subsequently, samples were snap frozen at -196°C in liquid nitrogen and stored at -80°C until further analysis. All analyses were performed within 3 months after sample collection. Lactate production, and glucose and pyruvate consumption (n = 96: 4 replicates, 4 treatments, 3 wells per treatment with both an apical and a basolateral compartment) were determined by an ultrafluorometric assay of spent medium as described by Gardner & Leese (1990), with modifications by Guerif *et al.* (2013) using a Tecan microplate reader, Infinite® 200 Pro (Tecan Trading AG, Switzerland). Blank medium aliquots (with no cellular contact) were collected to calculate consumption/production and data were expressed as nmol/well/h. As differences in consumption or production data in the pre-exposure samples can only be due to cell number, these values were used to normalize postexposure data. Data were expressed as a relative increase over the 24h exposure period.

6. BOEC gene expression analyses

Gene expression analyses were performed using two BOEC-monolayers per treatment in 4 replicates. The extraction of total RNA from cells was carried out using TRIzol® reagent according to manufacturer's instructions. The isolated RNA was suspended in 1 ml of isopropanol for at least 20 minutes. Subsequently, the isopropanol was vaporized in a vacuum chamber and the RNA pellet was washed in 70% ethanol. Subsequently, mRNA was selected using the Dynabeads® mRNA DIRECT™ Micro Kit (Ambion®, Thermo Fisher Scientific Inc., Oslo, Norway) according to manufacturer's instructions with minor modifications (Bermejo-Alvarez *et al.* 2008). To eliminate potential contamination with genomic DNA, all samples were incubated with DNase, at 37°C for 30 min and at 90°C for 5 min (RQ1 RNase-Free DNase, Promega Corporation, Madison, USA). RNA concentration was quantified at a wavelength of 260 nm and purity was assessed by the 260/280 ratio (Eppendorf BioPhotometer, Eppendorf Iberica, Madrid, Spain). cDNA synthesis and qPCR analysis were performed as described earlier (Maillo *et al.* 2016) in accordance with MIQE guidelines (Bustin *et al.* 2009). Briefly, RT reaction was carried out following the manufacturer's instructions (Epicentre Technologies Corp., Madison, U.S.A.) using poly (T) primers, random primers, and MMLV High Performance Reverse Transcriptase enzyme in a total volume of 50µl to prime the RT reaction and to produce cDNA. Tubes were heated to 70°C for 5 min to denature the secondary RNA structure and then the RT mix was completed with the addition of 50 units of reverse transcriptase. Afterwards they were incubated at 25°C for 10 min to favour the annealing of random primers, followed by 37°C 60 min to allow the RT of RNA, and finally 85°C 5 min to denature the enzyme.

Primers (table 1) were designed using Primer-BLAST software (www.ncbi.nlm.nih.gov/tools/primersblast/) to span exon-exon boundaries when possible. All qPCR reactions were carried out in duplicate on the Rotorgene 6000 Real Time Cycler™ (Corbett Research, Sydney, Australia) by adding 2µl aliquot of each sample to the PCR mix (GoTaq® qPCR Master Mix, Promega Corporation, Madison, USA) containing the specific primers selected to amplify the genes listed in Table 1. Cycling conditions were 94°C for 3 min followed by 35 cycles of 94°C for

15 sec, 56°C for 30 sec, 72°C for 10 sec and 10 sec of fluorescence acquisition. Fold-changes in the relative gene expression of the target were determined using the equation $2^{-\Delta\Delta CT}$ (Livak & Schmittgen 2001) using *H2AZ*, *ACTB* and *GAPD* as endogenous controls.

Statistical analysis

Data are expressed as means \pm SEM and were analyzed using IBM SPSS Statistics version 23 for Windows, (Chicago, IL, USA). Gene expression data were analyzed using Sigma Stat (Jandel Scientific, San Rafael, CA) software package. Mean differences in mRNA transcript abundance, spent medium carbohydrate metabolites, albumin-flux data, TER data, FA-transfer and **FA-transporter expression data** among the experimental groups were compared with mixed model ANOVA and posthoc Bonferroni tests including the fixed effect of treatment, the random effect of the repeat and their interaction (excluded when not significant). For normality and equality of variance reasons, pyruvate and lactate data were log transformed prior to statistical analyses. Differences with *P-values* <0.05 were considered statistically significant.

Results

1. BOEC-integrity and monolayer permeability

The TER-measurements were expressed as 'relative TER-increase' by comparing pre- and post-NEFA-exposure measurements, as none of the treatments reduced TER to the extent that monolayer integrity was compromised (i.e. $<700\Omega\cdot\text{cm}^2$ (Chen *et al.* 2015)). Elevated NEFAs induced a significantly lower TER-increase regardless of the exposure direction (figure 2).

The maximum FITC-albumin concentration in the non-supplemented compartment of unseeded wells was 4.3 μM . This flux was irrespective of assay direction and was correlated to the maximum FITC-albumin decrease in the opposite albumin supplemented compartment. The maximum flux (i.e. concentration of FITC-albumin in the non-supplemented compartment) observed in the unseeded wells was, therefore maximum 28.67% of the initial FITC-albumin concentration in the supplemented compartments at the beginning of the assay (i.e. 15 μM). Regardless of the treatment, when basal to

apical flux was observed in seeded wells, the maximum FITC-albumin concentration in the non-supplemented compartment of the control wells was 0.51 μ M (or 3.4%). When apical to basal flux was observed, the maximum flux was 1.8% of the initial FITC-albumin at the beginning the assay; as the maximum FITC-albumin concentration in the non-supplemented compartment of the control wells was 0.27 μ M. Only APICAL NEFA significantly increased the proportion of FITC transfer (3.8%) across the membrane ($P < 0.05$, figure 3) compared to controls, and only in basal to apical assay direction. Overall, albumin flux from the basal to the apical compartment was approximately two-times higher than that seen in the opposite direction. When the FITC transfer direction was inverted (to 'apical to basal') no treatment effects could be observed ($P > 0.05$).

2. BOEC NEFA transfer capacity

2.1 Total FA-concentration

In BASAL NEFA a 19% (or 122.5 \pm 4.3 μ M) reduction of total FA-content in the supplemented compartment could be detected after 24h exposure. In parallel, there was a 21% (or merely 12.7 \pm 1.4 μ M) rise in FA content in the apical chamber compared to the initial concentrations. By contrast, in APICAL NEFA total FA content fell by 53.4% (334.2 \pm 28.2 μ M) with no FA-transfer detected in the basal chamber.

2.2 FA-profiling per FA-fraction (free or esterified)

To specify the transfer, the total FA-concentrations were separated in individual FAs and classified as free or bound, esterified FAs (triglycerides, cholesterol esters and phospholipids). For both APICAL and BASAL NEFA, significant differences in total FA could only be found in the free FA-fraction. In BASAL NEFA, the significantly increased FAs in the non-supplemented, apical compartment were C16:0 (56.0 \pm 20.0%, $P = 0.042$), C18:0 (60.0 \pm 27.0%, $P = 0.098$) and C18:1 (33.5 \pm 6.0%, $P = 0.082$) in the total FA-fraction, while in the free, unbound fraction C14:0 (58.0 \pm 27.8%, $P = 0.035$), C16:1-cis-9 (81.1 \pm 19.3%, $P = 0.002$), C18:1-cis-9 (72.2 \pm 3.9%, $P = 0.017$) and C18:1-cis-11 (30.8 \pm 7.0%, $P = 0.004$) were found to be significantly increased.

In APICAL NEFA no differences in FA-increase could be detected in the non-supplemented compartment, as no FA-transfer was observed ($P>0.05$).

3. Intracellular lipid accumulation

Apical addition of NEFA caused an increased accumulation of neutral lipid droplets compared to other treatments (figure 4). Numerous lipid droplets were observed in the cytoplasm, and distributed evenly across the BOEC-monolayer. By contrast when NEFA was added to the basal compartment there was only limited lipid droplet accumulation in the BOECs. No lipid droplets were observed in the control groups.

4. BOEC fatty acid transporters

Fatty acid translocase/CD36 protein expression was upregulated in APICAL NEFA with 54.35% and 50.08% compared to BASAL NEFA and CONTROL conditions, respectively ($P<0.001$). Both APICAL and BASAL NEFA showed similar FABP3 expression, and were upregulated compared to CONTROLS by an average of 58.15% ($P<0.001$). CAV1 expression in APICAL NEFA was increased with 46.69% ($P<0.001$) and 52.90% ($P<0.001$) compared to BASAL NEFA and CONTROLS, respectively (figure 5).

5. BOEC energy metabolism: glucose, lactate and pyruvate concentrations

Under untreated conditions, BOECs depleted 49.91 ± 3.61 nmol/well/h of glucose from the apical compartment and 55.54 ± 10.82 nmol/well/h from the basal compartment. In addition, 35.69 ± 5.04 nmol/well/h of pyruvate was depleted from the apical compartment and 38.87 ± 7.16 nmol/well/h from the basal compartment. BOECs released 141.21 ± 8.31 nmol/well/h of lactate into the apical chamber and 152.58 ± 5.33 nmol/well/h into the basal compartment.

Twenty four hours after application of NEFA treatments, mean glucose release rose to of 77.36 ± 3.54 nmol/well/h in the apical compartment and 139.26 ± 35.81 nmol/well/h in the basal chamber. Pyruvate depletion from the apical compartment was largely unchanged in response to NEFA addition (34.76 nmol/well/h), although depletion from the basal compartment rose to 51.36 ± 8.34

nmol/well/h. Lactate appearance in the apical compartment was 154.92 ± 14.42 nmol/well/h and in the basal compartment 190.32 ± 11.99 nmol/well/h (figure 6).

No differences among the treatments could be detected.

6. BOEC gene expression analysis

The effects of BOEC NEFA exposure on the expression profile of genes involved in apoptosis (figure 7A), oxidative stress and specific BOEC-function (figure 7B) related genes was subsequently investigated. Addition of NEFA to the apical compartment led to increased expression of *BCL2*, compared to basal addition and control groups ($P < 0.01$), the consequence of which was to reduce the ratio of *BAX/BCL2* ($P < 0.01$). Stress adaptor protein, *SHC1*, was upregulated in response to apically-administered NEFA ($P < 0.05$), although this was also apparent in the SOLVENT CONTROL ($P < 0.01$). In addition, expression of *SOD1* was upregulated in response to apical administration of NEFA ($P < 0.05$). Expression of *OVGP1* (oviduct specific glycoprotein expression), *ESR1* (estrogen receptor expression) and *FOXJ1* (ciliogenesis) were all unchanged in response to NEFA and regardless of the exposure direction. Next, the impact of NEFA exposure on genes related to energy metabolism (figure 7C and 7D) was examined. mRNA expression of *G6PD* was downregulated after addition of NEFA to the apical chamber ($P < 0.05$) but upregulated when NEFA was added to the basal compartment ($P < 0.05$). The expression of *CPT1B* ($P < 0.05$) and *ACSL1* ($P < 0.05$) transcripts were upregulated while *ACACA*-expression ($P < 0.05$) was decreased in response to apical addition of NEFA.

Expression of BOEC FA-transporters resulted in upregulated *CAV1* ($P < 0.001$) expression in APICAL NEFA compared to other treatments (figure 7E). Overall, fold changes were low except for *BCL2* and *CAV1*.

Discussion

In this study, we hypothesized that elevated serum NEFA concentrations alter BOEC physiology, and more specifically BOEC metabolism and barrier function, potentially affecting the zygote's micro-environment. Hereto, PCC-system with hanging inserts was used to approach the BOECs in a most physiologically relevant manner (Fotheringham *et al.* 2011).

Overall, data indicate that APICAL NEFA resulted in an increased FITC-albumin-flux from the basal to the apical compartment. This increased monolayer permeability was also associated with reduced monolayer growth as suggested by slower increasing TER-values from Day 9 to 10. In BASAL NEFA, NEFA-concentrations decreased in the basal compartment with a concomitant increase in the apical chamber indicating limited FA-transfer. While apical FA-administration resulted in the increased lipid droplet formation and no transfer to the basal compartment. Depletion of carbohydrate metabolites seemed mostly active in the basal compartment, regardless of the treatments, substantiating the distinct effects of cellular polarity on the use of energy substrates in the culture system. Furthermore, APICAL NEFA induced anti-apoptotic and anti-oxidative pathways as suggested by increased expression of *BCL2* and *SOD1*, and may stimulate BOEC-lipid metabolism through increased intracellular FA-uptake (\uparrow *CAV1* and \uparrow FA-transporter protein expression CD36, FABP3 and *CAV1*), and upregulation of *CPT1B* and *ACSL1*. To our knowledge, the present study is the first to attempt a deeper understanding in the characteristics of BOECs under the influence of elevated NEFAs, hereby confirming cell polarity within the culture system and localizing different FA-transporters.

Characterization of **monolayer integrity** by means of TER-measurements resulted in ongoing increase in TER-values during the NEFA exposure period due to continuous cell growth (Jordaens *et al.*, 2015). In rat mammary epithelium, similar effects were observed and were considered to result from palmitic and stearic acid exposure (Wicha *et al.*, 1979). Data furthermore, indicated that APICAL NEFA resulted in reduced TER-increase during the 24h NEFA-exposure period and therefore decreased the tightness of intercellular cell contact (Chen *et al.* 2015). These data were supported by the **monolayer permeability** assessment using FITC labeled albumin. Here, only APICAL NEFA resulted in an increased FITC-albumin flux suggesting increased monolayer permeability and reduced monolayer tight junction quality (Anderson & Van Itallie 2009) in this treatment. Earlier, Roche *et al.* (2001) made similar observations in Caco2-cells, and reported that both TER, permeability and expression of tight junctions in Caco2-cells decreased due to elevated FAs and the tight junction modulating capacity of NEFAs. Considering the apical positioning of tight junctions between adjacent

cells, the increased monolayer permeability in APICAL NEFA of our study, may result from a more intense NEFA/tight junction contact in this treatment. The effects on permeability here observed, however, were limited specifically to the basal to apical albumin flux only. When the assay direction was inverted, total flux did not show any treatment effects. Apical to basal albumin flux was, however, lower compared to basal to apical flux, suggesting the oviductal lining to be still intact. It may also suggest intracellular uptake of the albumin in the apical to basal assay direction considering the equal amounts of albumin decrease in the supplemented compartments (see figure 8) in both assay directions, which can be explained by the expression of albumin binding cell surface receptors on the apical cell side of the oviduct only (Argaves & Morales 2004).

These findings and unpublished fluorescence microscopic imaging may, therefore, question the accuracy of the apical to basal assay direction as permeability parameter, but do provide us with interesting considerations when assessing the FA-transfer data.

FA-transfer across the BOEC-monolayers in BASAL NEFA showed a 19.5% FA-decrease in the supplemented, basal compartment and a 21.1% increase in the opposite, apical compartment. The absolute values of the transfer, however, suggest that only a minor proportion of the FAs are transferred from the basal to the apical compartment and substantiate the concept of a potential gatekeeper function of the oviduct. Intervening with transfer of detrimental metabolites to the oviductal lumen may thus be considered as an embryoprotective mechanism. When observing the transferred FAs in closer detail, we determined that all transferred FAs were unbound FAs and that it was mostly oleic and palmitic acid that could be transferred to the apical compartment. These data indicate that FA transfer **might be a selective process with a distinct active component for FA-uptake** (Glatz *et al.* 2010). Gas chromatographic analysis also revealed non-supplemented FAs to be present in the luminal chamber, suggesting some degree of metabolic modification. For example, the presence of C14:0, which was not added basally, may be indicative for *de novo* synthesis or conversion of C16:0 and C18:0 through partial oxidation (Lopaschuk *et al.* 2010). The presence C16:1-cis-9 may be a consequence of desaturation of PA, and C18:1-cis-11 from elongation

(Jakobsson *et al.* 2006). Therefore, not only transfer but also **FA metabolism** could be detected in this treatment (figure 9 for conceptualization). In contrast to this, when NEFA was added to the apical chamber, there was no subsequent appearance in the basal compartment. The FA-concentration in the apical supplemented compartment did, however, decrease by more than 50% over a 24h-timespan. The reduced apical FA-concentration, without signs of FA-transfer, suggests intracellular **FA-uptake for storage in lipid droplets**. Indeed, an increased accumulation of cytoplasmic lipid droplets in BOECs was observed in this treatment using Bodipy staining. The differences in lipid accumulation between the treatments was so apparent that no further quantification steps were undertaken. Cnop *et al.* (2001) observed lipid droplet formation in rat pancreatic cells and suggested cellular triglyceride accumulation as a cytoprotective mechanism against FA-induced lipotoxicity. In our current data, FA deposition in neutral lipid droplets was most abundantly observed in APICAL NEFA. BASAL NEFA showed lipid droplets to a limited extent, while lipid accumulation was completely absent in the CONTROL and SOLVENT CONTROL. On the basal cell side FABPs require non-albumin bound FAs for intracellular FA-uptake, which requires lipoprotein lipases that are typically expressed by endothelium (Glatz *et al.* 2010). These lipases are not present in our experimental design and may elucidate the lack of lipid accumulation in BASAL NEFA as most supplemented NEFAs in our experiments are albumin bound. The apical cell side, on the other hand and as mentioned above, typically expresses **caveolins**, megalins, cubilins, and lipoproteins allowing albumin bound FA-endocytosis (Argaves & Morales 2004; **Moestrup and Verroust, 2001**), facilitating cellular uptake of NEFA/albumin complexes from the luminal chamber in our experimental setting. **The presence (and abundance) of these transporters was confirmed in the current *in vitro* model through immunolabelling of BOEC FA-transporters and may elucidate the quantitative difference in lipid droplets observed between treatments. In this respect, CAV1 mRNA transcript abundance was upregulated in APICAL NEFA compared to other treatments, which resulted in increased translation of CAV1. FAT/CD36 and FABP3 showed similar FA-transporter expression in APICAL NEFA, however, no differences in mRNA transcripts could be detected when comparing different treatments. The**

latter might be explained by the increased use of the transcripts for translation with limited *de novo* transcriptional activity during the time period investigated (24h) as seen in early embryos (Robert, 2010). Interestingly, CD36 transporters are typically expressed in tissues that favor high FA-metabolism, as seen in mammary glands (Spitsberg *et al.*, 1985), but also metabolic conditions have shown to alter FA-utilization and FA-transporter expression as observed in adipocytes of diabetic rats (Berk *et al.*, 1997) and as simulated in the current experimental setting.

The fact that yet a few lipid droplets could be detected in BASAL NEFA can be accounted to the limited FA-transfer to the apical compartment in this treatment. Furthermore, these observations suit our findings made in the permeability assay where intracellular albumin uptake could only be observed when the fluorescent albumin was supplemented in the apical compartment. Complementary to these findings, BASAL NEFA treatment resulted in little to no differences in mRNA transcript abundance in the selected genes regarding lipid metabolism, possibly since the administered FAs are not taken up or partly redirected to the apical compartment. Gene expression analysis in APICAL NEFA, otherwise, resulted in increased lipid oxidation and reduced lipid synthesis. These data are suggestive for increased lipid metabolism of BOECs. However, and due to the abundance of the supplemented FAs, the supply may surpass the FA metabolism rate. Hereto, lipid storage may be employed as an adaptive tool to fulfill mitochondrial energy supply without hindering redox status and by reducing the amount of lipotoxic intermediates (Aon *et al.* 2014). This mechanism not only protects the cells from NEFA's detrimental effects but may also 'purify' the oviductal micro-environment. The environmental conditions for optimal embryo growth can thus be significantly improved, which is crucial considering the critical changes the embryo undergoes during its stay in the oviduct (Latham & Schultz 2001, Inbar-Feigenberg *et al.* 2013).

Analysis of spent medium for **BOEC-carbohydrate metabolites** did not reveal any significant differences in consumption of glucose or pyruvate, nor in production of lactate. In this respect, data are consistent with BOEC-transcriptome data. Regarding the genes selected for assessment of BOEC-energy metabolism, only *G6PD* transcript abundance showed significant differences: *G6PD* was

downregulated in APICAL NEFA and upregulated in BASAL NEFA, however, none of the other glucose-metabolism-related genes were affected. This suggests that glucose may be increasingly directed towards the pentose phosphate pathway in BASAL NEFA but the overall consumption was not affected. Regardless of the treatment, glucose uptake was most apparent in the basal, serum compartment, shifting glucose metabolites such as lactate in the apical compartment. *In vivo* BOECs are also provided with glucose via the serum (Leese. 1988): our findings therefore support the natural conditions. Earlier experiments (Jordaens *et al.* 2015), however, indicated that during the 24h exposure window, BOEC-monolayers showed continuous growth. In the current study, similar effects have been observed in increasing TER-values and elevated post-exposure glucose consumption in control groups. The latter were therefore normalized using pre-exposure data from the controls to minimize false interpretation. BOEC monolayers also showed an altered mitotic capacity, altered migration capacity and modified functionality due to elevated NEFAs (Jordaens *et al.*, 2015), which may easily mask turnover differences. In other cell types, similar NEFA-effects have been observed. Rat hepatocytes showed increased apoptosis due to steatosis after OA and PA exposure (Ricchi *et al.* 2009), pancreatic B-cells in rats were hyperplastic with morphological abnormalities under the influence of FAs (Milburn *et al.* 1995), and mouse embryos lacked cell proliferation capacity and showed a reduced developmental competence (Nonogaki *et al.* 1994). Interpretation of the current glucose, pyruvate and lactate turnover data should therefore be done with caution as the NEFA-conditions are known to affect monolayer characteristics. This is further supported by data on **gene expression** since we observed increased expression of genes related to FA-uptake, *CAV1* in APICAL NEFA. Caveolins are membrane proteins, typically expressed at the apical cell side, involved in clathrin independent endocytosis of proteins and lipids (Nabi and Le, 2003). Upregulation of these proteins in the presence of FA-abundance may elucidate the increased intracellular lipid uptake. Furthermore, upregulation of lipid metabolism β -oxidation (\uparrow *CPT1* and *ACSL1*) in this treatment, with downregulation of FA-synthesis related genes (\downarrow *ACACA*), appears to confirm our theory on embryo-protective “purification” of the oviduct micro-environment. The excess of FAs presented to the cells

apically may therefore be consumed as a metabolic fuel, while *de novo* FA-synthesis may be limited (Aon *et al.* 2014). In most tissues *de novo* FA-synthesis is of minor importance as the cellular requirements are predominantly met through FA-supply via the blood. Increased levels of circulating FAs inhibit FA-synthesis (Weis *et al.* 1986) and may result in decreased transcriptional activity of *ACACA*, as seen in the current data. The excessive FA-oxidation may also prompt to increase oxidative stress (Aon *et al.* 2014) in BOECs. The upregulation of *BCL2* and *SOD1* in APICAL NEFA may therefore be a direct reaction of BOECs to NEFA-exposure, increasing the cells' anti-oxidative and anti-apoptotic capacity. Harvey *et al.* (1995) and Tse *et al.* (2008) made similar observations in embryo/BOEC cocultures and may further explain BOEC's embryo protective capacity.

Ultimately, our findings may contribute to the concept that elevated NEFAs may modify the composition of the oviduct luminal fluid and alter the pre-implantation embryo's micro-environment. However, specific modifications were made to the experimental design. In this respect, NEFA-exposure was limited to 24h, whereas, *in vivo* NEFA concentrations are elevated over longer periods (Butler *et al.* 2003). Prolonged *in vitro* FA-incubation was, however, in other cell types associated with a significant decrease in cell viability (Ricchi *et al.* 2009). Furthermore, even acute NEFA exposure induced negative effects on BOECs and remains the only option to solely observe the direct cellular effects of NEFAs. Also, the use of serum for optimal cell attachment compromised the definition of the culture conditions. To minimize serum-effects, concentrations were contained to 5%, and the serum was analyzed for NEFA-content prior to use. Further *in vivo* studies are required to investigate the changes in the oviduct luminal fluid associated with maternal metabolic disorders, and how they may affect the micro-environment of the pre-implantation embryo. Nonetheless, our *in vitro* findings provide novel insights into the understanding of oviduct interactions with FAs.

In conclusion, elevated NEFAs affect BOEC metabolism and barrier function in a polarity dependent manner. In this respect, BOECs in BASAL NEFA potentially shield the luminal environment from elevated NEFAs by allowing only a limited amount of FAs to be transferred from the basal to the apical compartment. While BOECs in APICAL NEFA may clear the micro-environment of the pre-

implantation embryo from NEFAs through increased monolayer permeability, intracellular lipid accumulation and **FA metabolism**. Overall, the oviduct may modulate its micro-environment in favor of the early embryo by alleviating potential lipotoxic effects.

Declaration of interest

We declare that there is no conflict of interest that could be perceived as prejudicing the impartiality of the research reported.

Funding

This research did not receive any specific grant from any funding agency in the public, commercial or not-for-profit sector.

Acknowledgements

The authors acknowledge Els Merckx and Silke Andries, of the University of Antwerp Gamete Research Center, for their outstanding technical assistance throughout the experiments, and the AML 'Antwerps Medisch Labo' for the NEFA-analyses.

References

Aardema H, Vos PLAM, Lolicato F, Roelen BA, Knijn HM, Vaandrager AB, Helms JB & Gadella BM 2011 Oleic acid prevents detrimental effects of saturated fatty acids on bovine oocyte developmental competence. *Biology of Reproduction* **85** 62-69.

Ackman RG & Sipos JC 1964 Application of specific response factors in the gas chromatographic analysis of methyl esters of fatty acids with flame ionization detectors. *Journal of the American Oil Chemists' Society* **41** 377-378.

Anderson JM & Van Itallie CM 2009 Physiology and function of the tight junction. *Cold Spring Harbor Perspectives in Biology* **1(2)** a002584.

Aon MA, Bhatt N & Cortassa SC 2014 Mitochondrial and cellular mechanisms for managing lipid excess. *Frontiers in Physiology* **5**: 282 doi:[10.3389/fphys.2014.00282](https://doi.org/10.3389/fphys.2014.00282).

Argaves WS & Morales CR 2004 Immunolocalization of cubilin, megalin, apolipoprotein J and apolipoprotein A-I in the uterus and oviduct. *Molecular Reproduction and Development* **69** 419-427.

Berk PD, Zhou SI, Kiang CL, Stump D, Bradbury M, Isola LM 1997 Uptake of long chain free fatty acids is selectively upregulated in adipocytes of Zucker rats with genetic obesity and non-insulin-dependent diabetes mellitus. *Journal of Biological Chemistry* **272**(13) 8830-8835.

Bermejo-Álvarez P, Rizo, D, Rath D, Lonergan P & Gutierrez-Adan A 2008 Epigenetic differences between male and female bovine blastocysts produced in vitro. *Physiological Genomics* **32**(2) 264-272.

Bustin SA, Bene, V, Garson JA, Hellemans J, Higgett J, Kubista M, Mueller R, Nolan T, Pfaffl MW, Shipley GL, Vandesompele J & Wittwer CT 2009 The MIQE Guidelines: Minimum Information for publication of Quantitative real-time PCR Experiments. *Clinical Chemistry* **55**(4) 611-622.

Butler ST, Marr AL, Pelton SH, Radcliff RP & Lucy MC 2003 Insulin restores GH responsiveness during lactation induced negative energy balance in dairy cattle: effects of expression of IGF-I and GH receptor-1A. *Journal of Endocrinology* **176** 205-217.

Chang YS, Munn LL, Hillsley MV, Dull RO, Yuan J, Lakshminarayanan S, Gardner TW, Jain RK & Tarbell JM 2000 Effect of vascular endothelial growth factor on cultured endothelial cell monolayer transport properties. *Microvascular Research* **59** 265-277.

Chen S, Einspanier R & Schoen J 2015 Transepithelial electrical resistance (TEER): a functional parameter to monitor the quality of oviduct epithelial cells cultured on filter supports. *Histochemistry and Cell Biology* **144**(5) 509-515.

Cnop M, Hannaert JC, Hoorens A, Eizirik DL & Pipeleers DG 2001 Inverse relationship between cytotoxicity of free fatty acids in pancreatic islet cells and cellular triglyceride accumulation. *Diabetes* **50** 1771-1777.

Fotheringham S, Levanon K & Drapkin R 2011 Ex vivo culture of human primary fallopian tube epithelial cells. *Journal of Visualized Experiments* **51**: e2728, doi:[10.3791/2728](https://doi.org/10.3791/2728).

Gardner DK & Leese HJ 1990 Concentrations of nutrients in mouse oviduct fluid and their effects on embryo development and metabolism *in vitro*. *Journal of Reproduction and Fertility* **88** 361-368.

Glatz JF, Luiken JJ & Bonen A 2010 Membrane fatty acid transporters as regulators of lipid metabolism: implications for metabolic disease. *Physiological Reviews* **90**(1) 367-417.

Guerif F, McKeegan P, Leese HJ & Sturmey RG 2013 A simple approach for Consumption and Release (CORE) analysis of metabolic activity in single mammalian embryos. *PLoS One* **8**(8):e67834.

Harvey MB, Arcellana-Panlilio MY, Zhang X, Schultz GA & Watson AJ 1995 Expression of genes encoding antioxidant enzymes in preimplantation mouse and cow embryos and primary bovine oviduct cultures employed for embryo coculture. *Biology of Reproduction* **53**:532-540.

Inbar-Feigenberg M, Choufani S, Butcher DT, Roifman M & Weksberg R 2013 Basic concepts of epigenetics. *Fertility and Sterility* **99**(3) 607-615.

Jakobsson A, Westerberg R & Jacobsson A 2006 Fatty acid elongases in mammals: their regulation and roles in metabolism. *Progress in Lipid Research* **45**(3) 237-249.

Jordaens L, Arias-Alvarez M, Pintelon I, Thys S, Valckx S, Dezhkam Y, Bols PEJ & Leroy JLMR 2015 Elevated non-esterified fatty acid concentrations hamper bovine oviductal epithelial cell physiology in three different *in vitro* culture systems. *Theriogenology* **84** 899-910.

Jorritsma R, César ML, Hermans JT, Kruitwagen CLJJ, Vos PLAM & Kruijff TAM 2004 Effects of non-esterified fatty acids on bovine granulosa cells and developmental potential of oocytes *in vitro*. *Animal Reproduction Science* **81** 225-235.

Jungheim ES, Loudon ED, Chi MMY, Frolova AI, Riley JK & Moley KH 2011 Preimplantation exposure of mouse embryos to palmitic acids results in fetal growth restriction followed by catch-up growth in the offspring. *Biology of Reproduction* **85** 678-683.

Lash MM & Armstrong A 2009 Impact of obesity on women's health. *Fertility and Sterility* **91** 1712-1716.

Latham KE & Schultz R M 2001 Embryonic genome activation. *Frontiers in Bioscience* **6** 748-759.

Leese HJ 1988 The formation and function of oviduct fluid. *Journal of Reproduction and Fertility* **82** 843-856.

Leese HJ, Hugentobler SA, Gray SM, Morris DG, Sturmey RG, Whitear SL & Sreenan JM 2007 Female reproductive tract fluids: composition, mechanism of formation and potential role in the developmental origins of health and disease. *Reproduction, Fertility and Development* **20** (1) 1-8.

Leroy JLMR, Vanholder T, Delanghe JR, Opsomer G, Van Soom A & Bols PEJ 2004 Metabolite and ionic composition of follicular fluid from different-sized follicles and their relationship to serum concentrations in dairy cows. *Animal Reproduction Science* **80** 201-211.

Leroy JLMR, Vanholder T, Mateusen B, Christophe A, Opsomer G, de Kruif A, Genicot G & Van Soom A 2005 Non-esterified fatty acids in follicular fluid of dairy cows and their effect on developmental capacity of bovine oocytes *in vitro*. *Reproduction* **130** 485-495.

Leroy JLMR, Opsomer G, Van Soom A, Goovaerts IG & Bols, PEJ 2008a Reduced fertility in high-yielding dairy cows: are the oocyte and embryo in danger? Part I. The importance of negative energy balance and altered corpus luteum function to the reduction of oocyte and embryo quality in high-yielding dairy cow. *Reproduction in Domestic Animals* **43** 612-622.

Leroy JLMR, Van Soom A, Opsomer G, Goovaerts IG & Bols PEJ 2008b Reduced fertility in high-yielding dairy cows: are the oocyte and embryo in danger? Part II. Mechanisms linking nutrition and reduced oocyte and embryo quality in high-yielding dairy cows. *Reproduction in Domestic Animals* **43** 623-632.

Leroy JLMR, Van Hoeck V, Clemente M, Rizos D, Gutierrez-Adan A, Van Soom A, Uytterhoeven M & Bols PEJ 2010 The effect of nutritionally induced hyperlipidemia on *in vitro* bovine embryo quality. *Human Reproduction* **25**(3) 768-778.

Listenberger LL, Han X, Lewis SE, Cases S, Farese RV, Ory DS & Schaffer JE 2003 Triglyceride accumulation protects against fatty acid induced lipotoxicity. *Proceedings of the National Academy of Sciences* **100**(6) 3077-3082.

Livak KJ & Schmittgen TD 2001 Analysis of relative gene expression data using real-time quantitative PCR and the $2^{-\Delta\Delta C_t}$ method. *Methods* **25** 402-408.

Löfgren L, Ståhlman M, Forsberg GB, Saarinen S, Nilsson R & Hansson GI 2012 The BUME method: a novel automated chloroform-free 96-well total lipid extraction method for blood plasma. *Journal of Lipid Research* **53** 1690–1700 doi:10.1194/jlr.D023036.

Lopaschuk GD, Ussher JR, Folmes CDL, Jaswal JS & Stanley WC 2010 Myocardial fatty acid metabolism in health and disease. *Physiological Review* **90** 207-258.

Maillo V, Rizos D, Besenfelder U, Havlicek V, Kelly AK, Garrett M & Lonergan P 2012 Influence of lactation on metabolic characteristics and embryo development in postpartum Holstein dairy cows. *Journal of Dairy Science* **95** 3865-3876.

Maillo V, de Frutos C, O’Gaora P, Forde N, Burns GW, Spencer TE, Gutierrez-Adan A, Lonergan P & Rizos D 2016 Spatial differences in gene expression in the bovine oviduct. *Reproduction* **152**(1) 37-46.

Matoba S, O’Hara L, Carter F, Kelly AK, Fair T, Rizos D & Lonergan P 2012 The association between metabolic parameters and oocyte quality early and late post-partum in Holstein dairy cows. *Journal of Dairy Science* **95** 1257-1266.

Miessen K, Sharbati S, Einspanier R & Schoen J 2011 Modelling the porcine oviduct epithelium: a polarized *in vitro* system suitable for long-term cultivation. *Theriogenology* **76** 900-910.

Milburn JL Jr, Hirose H, Lee YH, Nagasawa Y, Ogawa A, Ohneda M, BeltrandelRio H, Newgard CB, Johnson JH & Unger RH 1995 Pancreatic B-cells in obesity: evidence for induction of functional, morphologic and metabolic abnormalities by increased long chain fatty acids. *Journal of Biological Chemistry* **270**(3) 1295-1299.

Moestrup SK and Verroust PJ 2001 Megalin- and Cubilin-mediated endocytosis of protein-bound vitamins, lipids, and hormones in polarized epithelia. *Annual Review of Nutrition* **21** 407-428.

Nabi and Le 2003 Caveolae/raft-dependent endocytosis. *The Journal of Cell Biology* **161**(4) 673-677.

Nonogaki T, Noda Y, Goto Y, Kishi J & Mori T 1994 Developmental blockage of mouse embryos caused by fatty acids. *Journal of Assisted Reproduction and Genetics* **11**(9) 482-488.

Ricchi M, Odoardi MR, Carulli L, Anzivino C, Ballestri S, Pinetti A, Fantoni LI, Marra F, Bertolotti M, Banni S, Lonardo A, Carulli N & Loria P 2009 Differential effect of oleic and palmitic acid on lipid accumulation and apoptosis in cultured hepatocytes. *Journal of Gastroenterology and Hepatology* **24** 830-840.

Rizos D, Carter F, Besenfelder U, Havlicek V & Lonergan P 2010 Contribution of the female reproductive tract to low fertility in postpartum lactating dairy cows. *Journal of Dairy Science* **93** 1022-1029.

Robert C 2010 Microarray analysis of gene expression during early embryo development: a cautionary overview. *Reproduction* **140**(6) 787-801.

Robker RL, Akison LK, Bennett BD, Thrupp PN, Chura LR, Russell DL, Lane M & Norman RJ 2009 Obese women exhibit differences in ovarian metabolites, hormones and gene expression compared with moderate-weight women. *Journal of Clinical Endocrinology and Metabolism* **94**(5) 1533-1540.

Roche HM, Terres AM, Black IB, Gibey MJ & Kelleher D 2001 Fatty acids and epithelial permeability: effect of conjugated linoleic acid on CaCo-2 cells. *Gut* **48** 797-802.

Spitsberg VL, Matitashvili E, Gorewit RC 1995 Association and coexpression of fatty acid binding protein and glycoprotein CD36 in the bovine mammary gland. *European Journal of Biochemistry* **230** 872-878.

Tahir MZ, George F, Donnay I 2011 Comparison of different membrane supports for monolayer culture of bovine oviduct epithelial cells. *BMC Proceedings* **5**(8): 117.

Tse PK, Lee YL, Chow WN, Luk JMC, Lee KF & Yeung WSB 2008 Preimplantation embryos cooperate with oviductal cells to produce embryothropic inactivated complement-3b. *Endocrinology* **149**(3) 1268-1276.

Valckx SDM, De Pauw I, De Neubourg D, Inion I, Berth M, Franssen E, Bols PEJ & Leroy JLMR 2012 BMI-related metabolic composition of the follicular fluid of women undergoing assisted reproductive treatment and the consequences for oocyte and embryo quality. *Human Reproduction* **27**(12) 3531-3539.

Valckx SDM, Van Hoeck V, Arias-Alvarez M, Maillou V, Lopez-Cardona AP, Gutierrez-Adan A, Berth M, Cortvrindt R, Bols PEJ & Leroy JLMR 2014 Elevated non-esterified fatty acid concentrations during in vitro murine follicle growth alter follicular physiology and reduce oocyte developmental competence. *Fertility and Sterility* **102**(6) 1769-1776.

Valckx SDM, De Bie J, Michiels ED, Goovaerts IG, Punjabi U, Ramos-Ibeas P, Gutierrez-Adan A, Bols PEJ & Leroy JL
2015 The effect of human follicular fluid on bovine oocyte developmental competence and embryo quality. *Reproductive Biomedicine Online* **30**(2) 203-207.

Van Hoeck V, Sturmey RG, Bermejo-Alvarez P, Rizos D, Gutierrez-Adan A, Leese HJ, Bols PEJ & Leroy JL
2011 Elevated non-esterified fatty acid concentrations during bovine oocyte maturation compromise early embryo physiology. *PLoS One* **6**(8):e23183.

Van Hoeck V, Leroy JL, Arias-Alvarez M, Rizos D, Gutierrez-Adan A, Schnorbusch K, Bols PEJ, Leese HJ & Sturmey RG
2013 Oocyte developmental failure in response to elevated nonesterified fatty acid concentrations: mechanistic insights. *Reproduction* **145** 33-44.

Velazquez MA, Parrilla I, Van Soom A, Verberckmoes S, Kues W & Niemann H
2010 Sampling techniques for oviductal and uterine luminal fluid in cattle. *Theriogenology* **73** 758-767.

Vlaeminck B, Braeckman T & Fievez V
2014 Rumen metabolism of 22:6n-3 in vitro is dependent on its concentration and inoculum size, but less dependent on substrate carbohydrate composition. *Lipids* **49** 517–525. doi:10.1007/s11745-014-3905-8.

Weis L, Hoffman G, Schreiber R, Andres H, Fuchs E, Korber E & Kolb H
1986 Fatty acid synthesis in man, a pathway of minor importance. Purification, optimal assay conditions and organ distribution of fatty acid synthase. *Biological Chemistry Hoppe-Seyler* **367** 905-912.

Wicha MS, Liotta LA, Kidwell WR
1979 Effects of free fatty acids on the growth of normal and neoplastic rat mammary epithelial cells. *Cancer Research* **39**: 426-435.

Wolff RL, Bayard CC & Fabien RJ
1995 Evaluation of sequential methods for the determination of butterfat fatty acid composition with emphasis on trans-18:1 acids. Application to the study of seasonal variations in french butters. *Journal of American Oil Chemists' Society* **72** 1471–1483 doi:10.1007/BF02577840.

Figure legends:

Figure 1: Experimental design to study the effects of NEFAs in a polarized cell culture system according to different exposure directions: C = control medium containing 0 μ M NEFA, SC = solvent control medium containing 0 μ M NEFA + 0.45% EtOH, NEFA = 720 μ M NEFA with 230 μ M PA+ 280 μ M SA+ 210 μ M OA. At Day 9 (pre-exposure samples) and 10 (post-exposure samples) spent media were collected. At Day 10 other outcome parameters in BOECs were assessed.

Figure 2: Relative TER-increase was calculated through comparison of pre- and post NEFA-exposure TER-measurements. ^{a,b} Different superscripts per bar indicate statistical significant differences ($P < 0.05$); *: $P = 0.05$.

Figure 3: The permeability assay showed FITC-albumin flux measured in the non-supplemented compartment after a 3h assay in which the FITC-albumin-flux from the basal to the apical compartment (A), and the flux from the apical to the basal compartment (B) were observed. ^{a,b} Different superscripts per bar indicate statistical significant differences ($P < 0.05$).

Figure 4: Lipid droplet analysis was performed using Bodipy 493/503 (green) to visualize intracytoplasmic droplets of neutral lipids and DAPI (blue) for staining nuclei. Monolayers from the CONTROL group (C) and SOLVENT CONTROL (D) showed no lipid droplets, while BOEC-monolayers from the APICAL NEFA group (A) clearly showed accumulation of lipids in the cells, and BASAL NEFA (B) displayed little to no lipid droplets. Images were made at 60x magnification using confocal microscopy.

Figure 5: Immunolabelling of specific fatty acid transporters was performed to visualize and quantify specific FA-transporter expression (green) per nucleus (blue). Fatty acid translocase CD36 (A), fatty acid binding protein 3 (FABP3) (B) and caveolin 1 (CAV1) (C) are presented with their respective negative controls and mean transporter fluorescence per nucleus in different treatments. Scale bars indicate 20 μ m. ^{a,b} Different superscripts per bar indicate statistical significant differences ($P < 0.05$).

Figure 6: Glucose (A) and pyruvate (C) consumption, and lactate (B) production (%) in spent medium were expressed as relative values of pre and post NEFA-exposure samples taken with a 24h interval and in different treatment groups. Full bars represent the apical compartment, dotted bars represent the basal compartment.

Figure 7: mRNA transcript abundance (\pm SEM) after qRT-PCR gene expression analyses. Genes are sorted based on function: A. Apoptosis, B. Oxidative stress and BOEC-function, C. BOEC-carbohydrate metabolism, D. BOEC-lipid metabolism, and E. FA-uptake. ^{a,b,c} Different superscripts per bar indicate statistical significant differences ($P < 0.05$)

Figure 8: The permeability assay showed a decrease in FITC-albumin concentrations measured in the albumin supplemented compartment after a 3h assay in both the basal to apical (A) and apical to basal (B) assay direction. ^{a,b} Different superscripts per bar indicate statistical significant differences ($P < 0.05$).

Figure 9: Graphic summary of the obtained results and conceptualization of fatty acid transfer across BOEC-monolayers as suggested in the experiments above. Red arrows indicate the FA-transfer: via paracellular transport the basally supplemented FAs (A) are directed to the apical oviductal lumen compartment as non-esterified FAs, where they can be internalized by the cells and directly used as an energy substrate or in case of abundance, stored in lipid droplets (B). Gene expression is altered to allow the cells metabolic adaptation and upregulated anti-oxidative and anti-apoptotic pathways after exposure to elevated NEFAs. Green arrows suggest the increased permeability from the basal to the apical compartment in APICAL NEFA, proposing the possibility that the oviductal micro-environment may be subjected to all kinds of metabolic changes. Nuclei are orange, secretory granules are blue, and lipid droplets are depicted in yellow. These data suggest cellular adaptation to changing environmental conditions.

Table 1: List of primers used showing primer sequences, fragment sizes, and gene bank accession numbers. GAPDH, H2AFZ and ACTB were used as endogenous controls.

Gene	Gene name	Primer sequence (5'-3')	Fragment size (bp)	Gene bank accession no.
ACACA	Acetyl-CoA carboxylase alpha	AAGCAATGGATGAACCTTCTTC GATGCCCAAGTCAGAGAGC	196	FN185963.1
ACSL1	Acyl-CoA synthetase long-chain family member 1	TGACTGTTGCTGGAGACTGG TGTGCTTCTTCTGTGCATG	250	NM_001076085.1
ACTB	Actin, beta	GAGAAGCTCTGCTACGTCG CCAGACAGCACCGTGTGG	264	AF191490.1
BAX	BCL2-Associated X Protein	CTGGAGCAGGTGCCTCAGGA ATCTCGAAGGAAGTCCAGCGTC	300	NM_001166486.1
BCL2	B-Cell CLL/Lymphoma 2	GGAGCTGGTGGTTGACTTTC CTAGGTGGTCATTCAGGTAAG	517	BC147863.1
CAV1	Caveolin 1	TCAGCCGTGTCTATTCC ATTTCTTTCTGCGTGTG	103	NM_174004.3
CD36	CD36 molecule, fatty acid translocase	GCTCCTTAAGCCATTCTTGGAT CACCAGTGTCAACGCACTTT	151	NM_001278621.1
CPT1B	Carnitine palmitoyltransferase 1B	CTGCCCGCTGGGAAATGCTGT CAGTCTCTCTCCCCGGGCTGG	332	NM_001034349.2
ESR1	Estrogen receptor 1	CCCGCCAAGTTCTGAGAATCC CAAGGCGTGCCACGTAGAAGT	159	NM_001001443.1
FABP3	Fatty acid binding protein 3	TTGTGCGGGAGATGGTTGA TGCCGAGTCCAGGAGTAGCC	147	NM_174313.2
FOXJ1	Forkhead box J1	AGCAAGGCCACCAAGATCACC CCGAGGCACCTTGATGAAGCAC	145	NM_001192076.1
GAPDH	Glyceraldehyde-3-phosphate dehydrogenase	ACCCAGAAGACTGTGGATGG ATGCCTGCTTACCACCTTC	247	NM_001034034.2
GPX1	Glutathione Peroxidase 1	GCAACCAGTTTGGGCATCA CTCGACTTTTGAAGAGCATA	116	NM_174076.3
G6PD	Glucose-6-phosphate dehydrogenase	CGCTGGGACGGGTGCCCTTCATC CGCCAGGCTCCCGCAGTTCATCA	347	NM_001244135.1
H2AFZ	H2A histone family, member Z	AGGACGACTAGCCATGGACGTGTG CCACCACCAGCAATTGTAGCCTTG	209	NM_174809
LDHA	Lactate dehydrogenase A	TTCTTAAGGAAGAACATGTC TTCACGTTACGCTGGACCAA	310	NM_174099.2
LPL	Lipoprotein lipase	ATTGCTCAGCATGGCTCGGAAG TCCCAGGGCCATACACTGACTG	309	NM_001075120.1
OVGP1	Oviductal glycoprotein 1	AAGAATGAGGCCAGCTCAC TGCCGAAGATTTGGGGTCTC	219	NM_001080216.1
SHC1	SHC (Src Homology 2 Domain Containing) Transforming Protein 1	GTGAGGTCTGGGGAGAAGC GGTTCCGACAAAGGATCACC	334	NM_001075305
SCL2A1	Solute carrier family 2 (facilitated glucose transporter) member 1 (former GLUT1)	CTGATCCTGGGTGCTTCAT ACGTACATGGGCACAAAACCA	68	NM_174602.2
SOD1	Superoxide dismutase 1, soluble	ATCATTGGCCGCACGATGGTG CCACAGGCCAAACGACTTCCAG	107	NM_174615
TJP1	Tight Junction Protein 1	AATCATCCGACTCCTCGTCG CCCAAACACAGCGCGTAAAA	255	XM_010817146.1
TP53	Tumor Protein P53	CTCAGTCCTTGCCATACTA GGATCCAGGATAAGGTGAGC	364	NM_174201.2

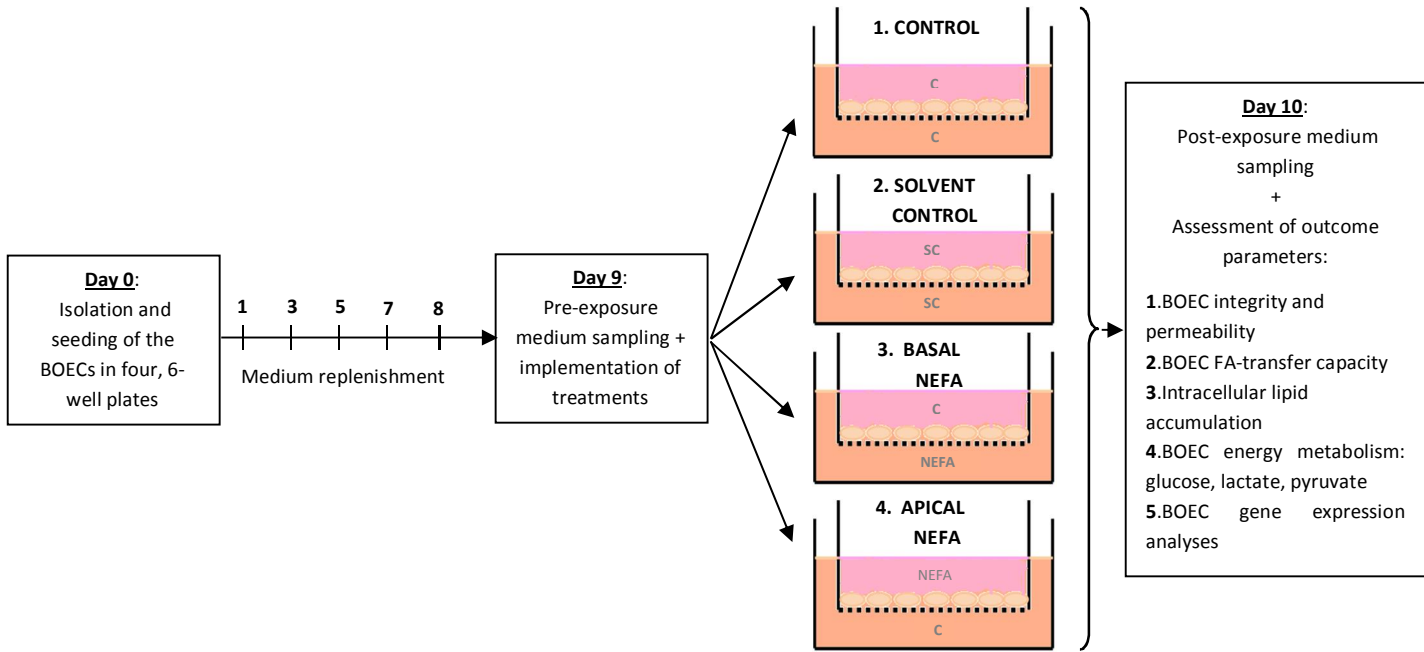


Figure 1

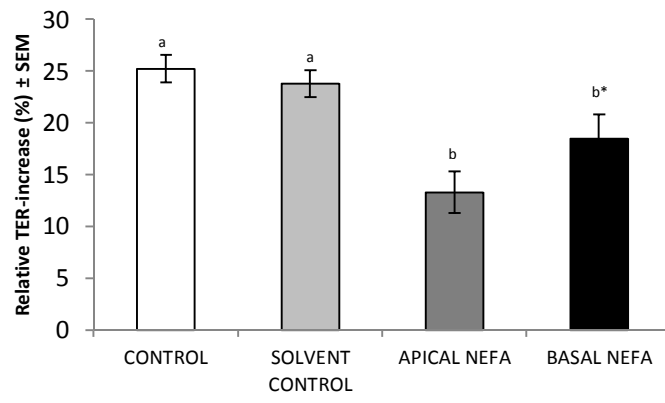


Figure 2

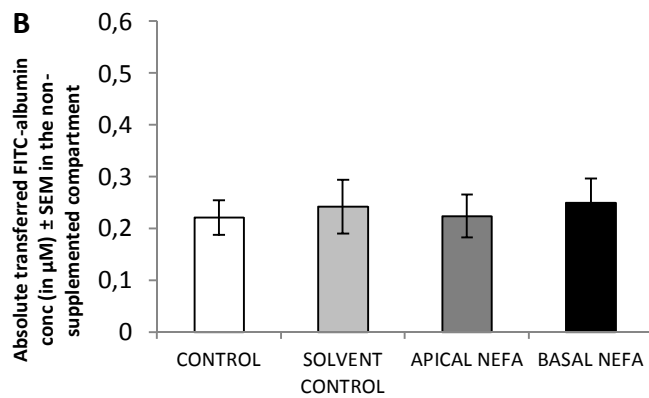
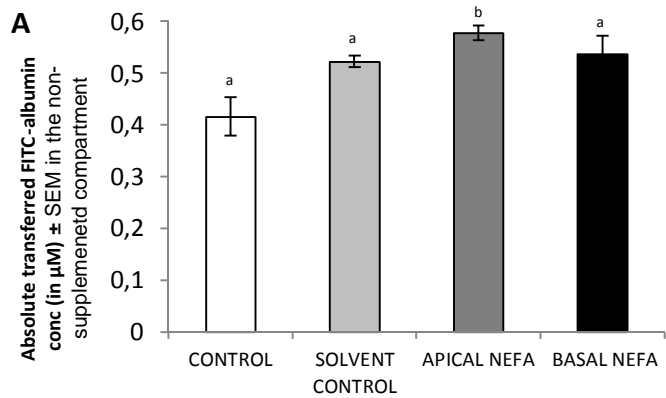


Figure 3

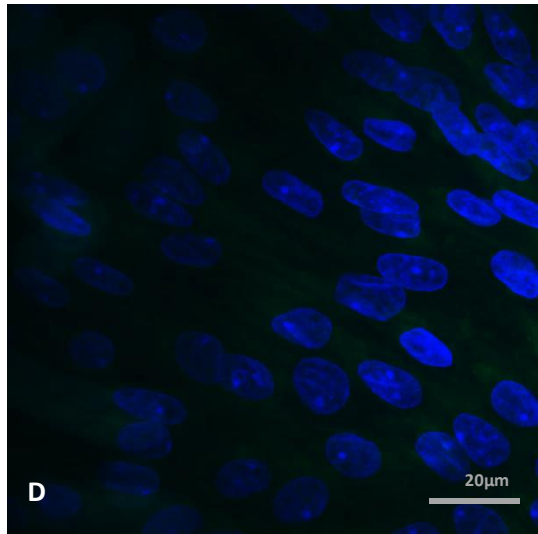
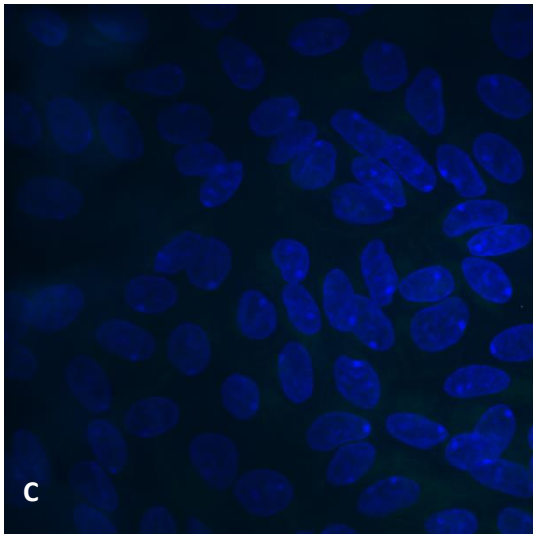
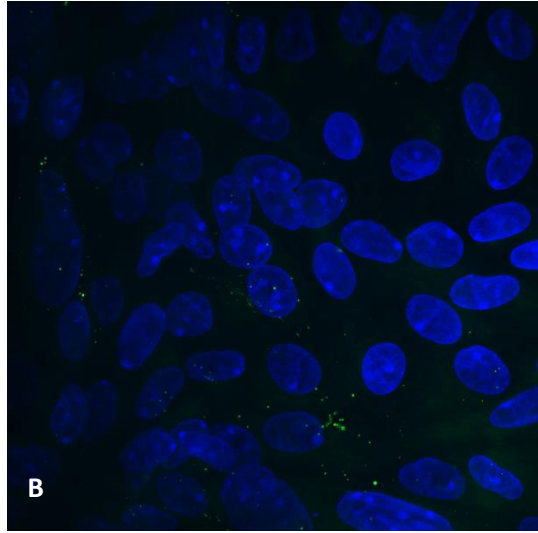
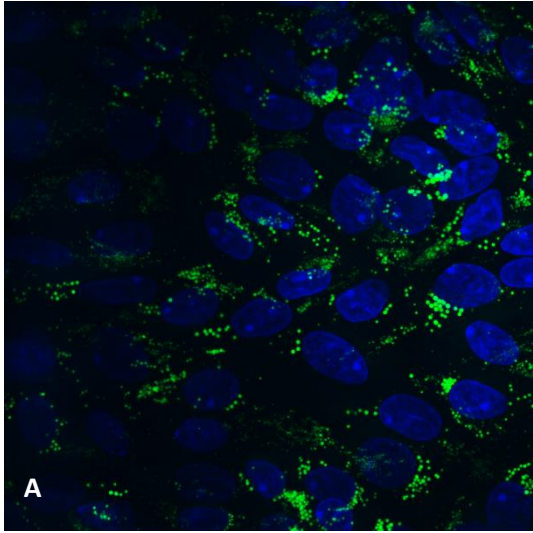
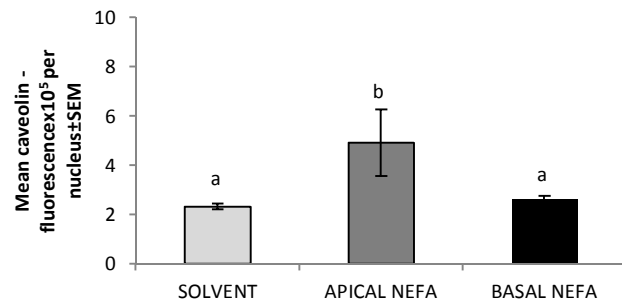
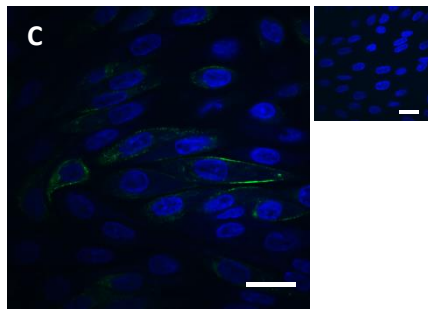
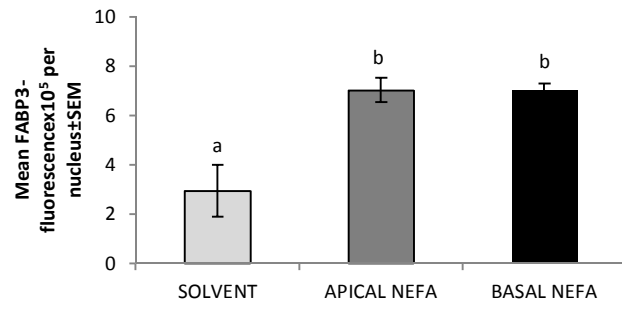
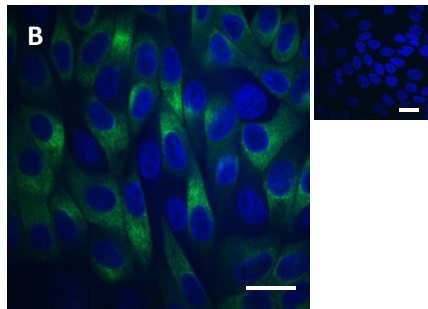
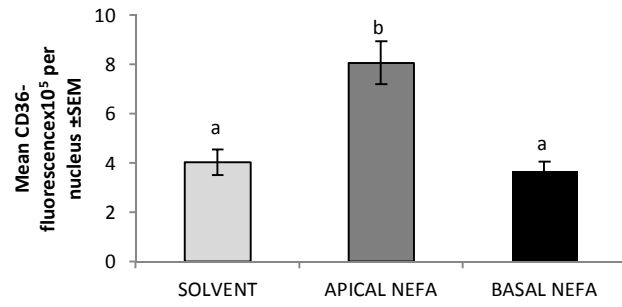
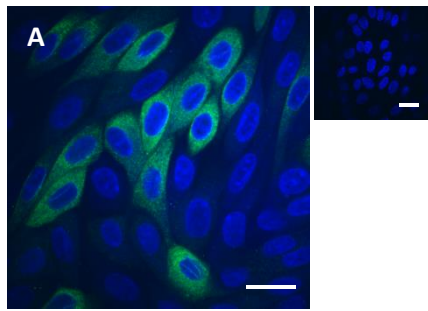


Figure 4



SOLVENT;
 APICAL NEFA;
 BASAL NEFA

Figure 5

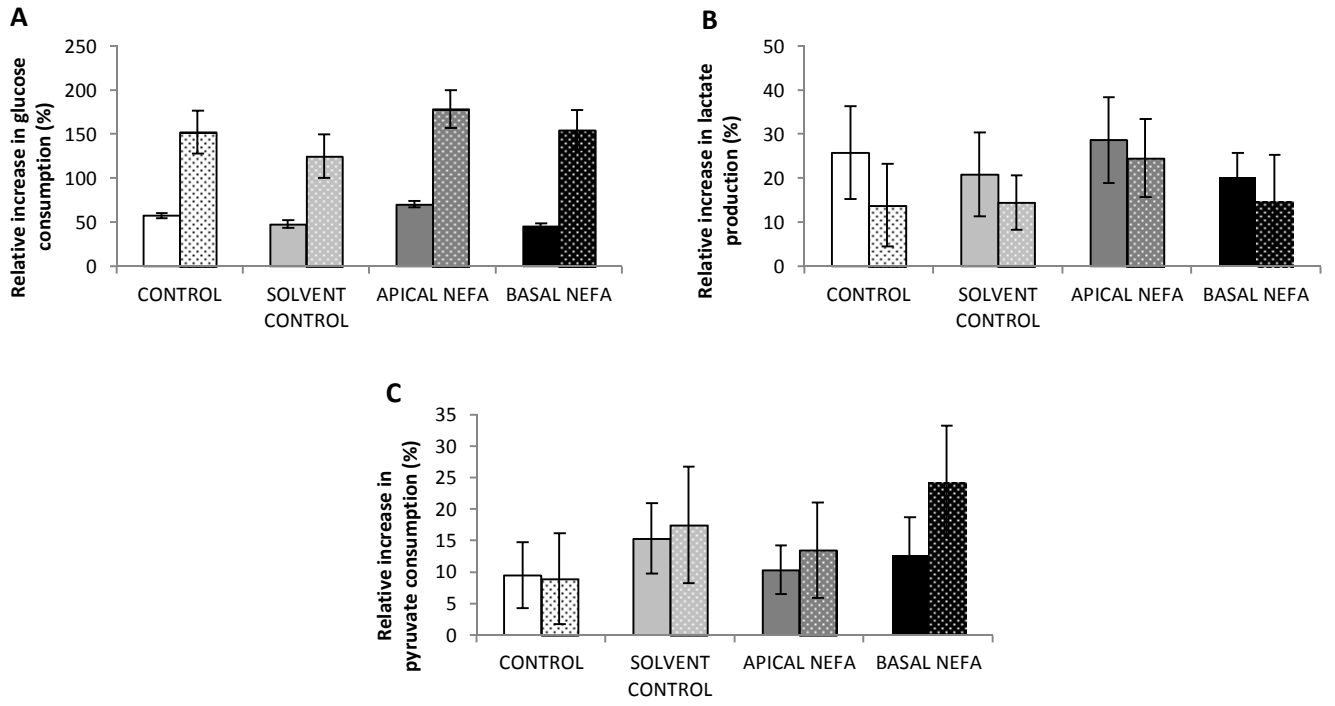


Figure 6

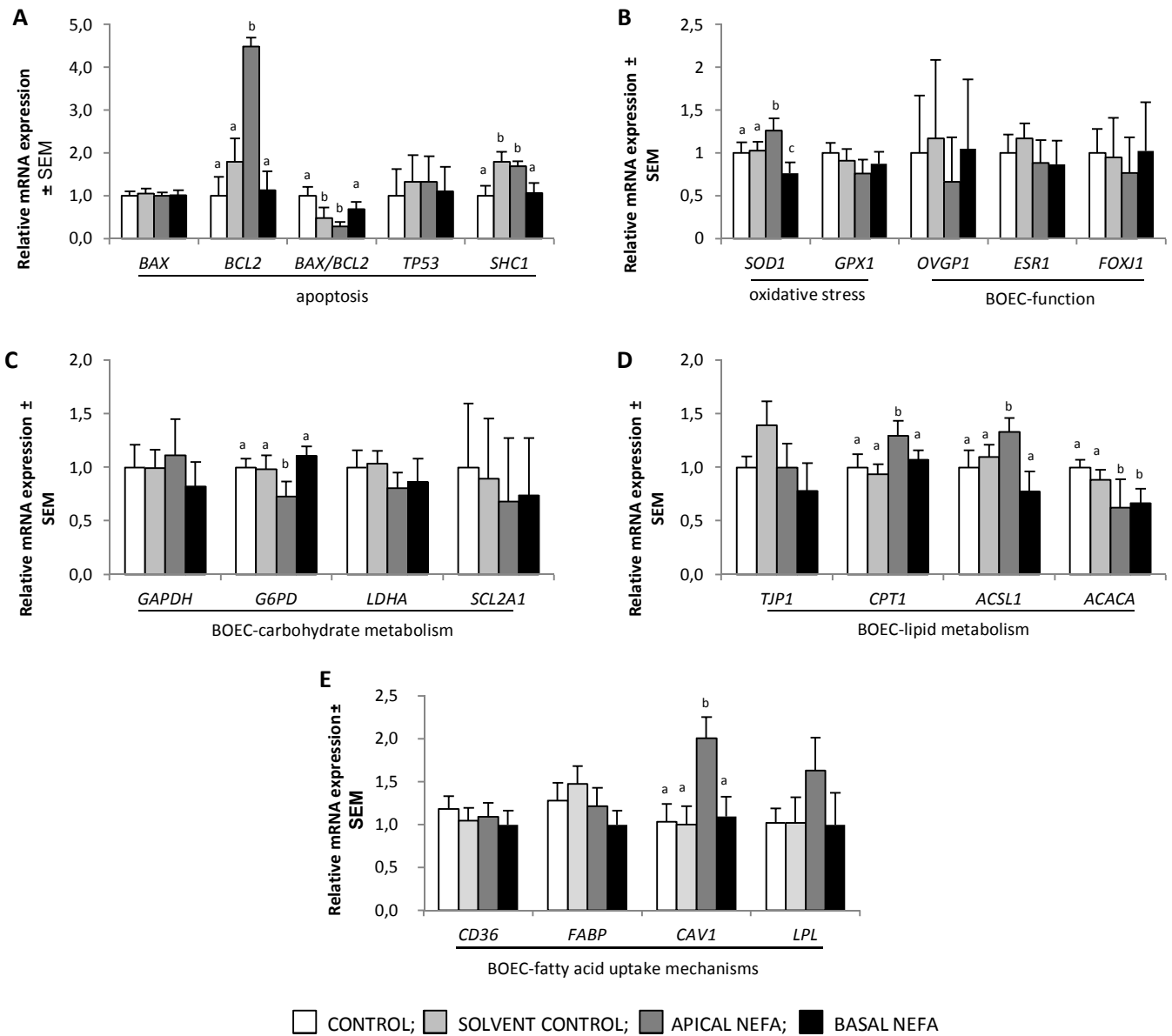


Figure 7

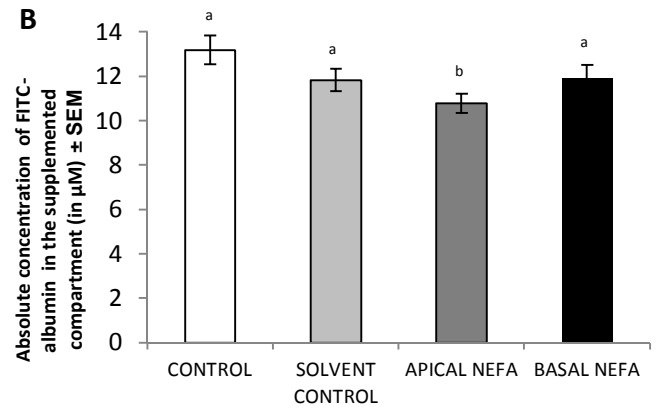
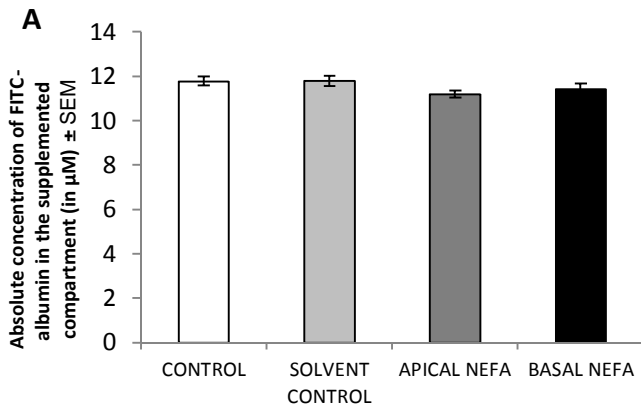
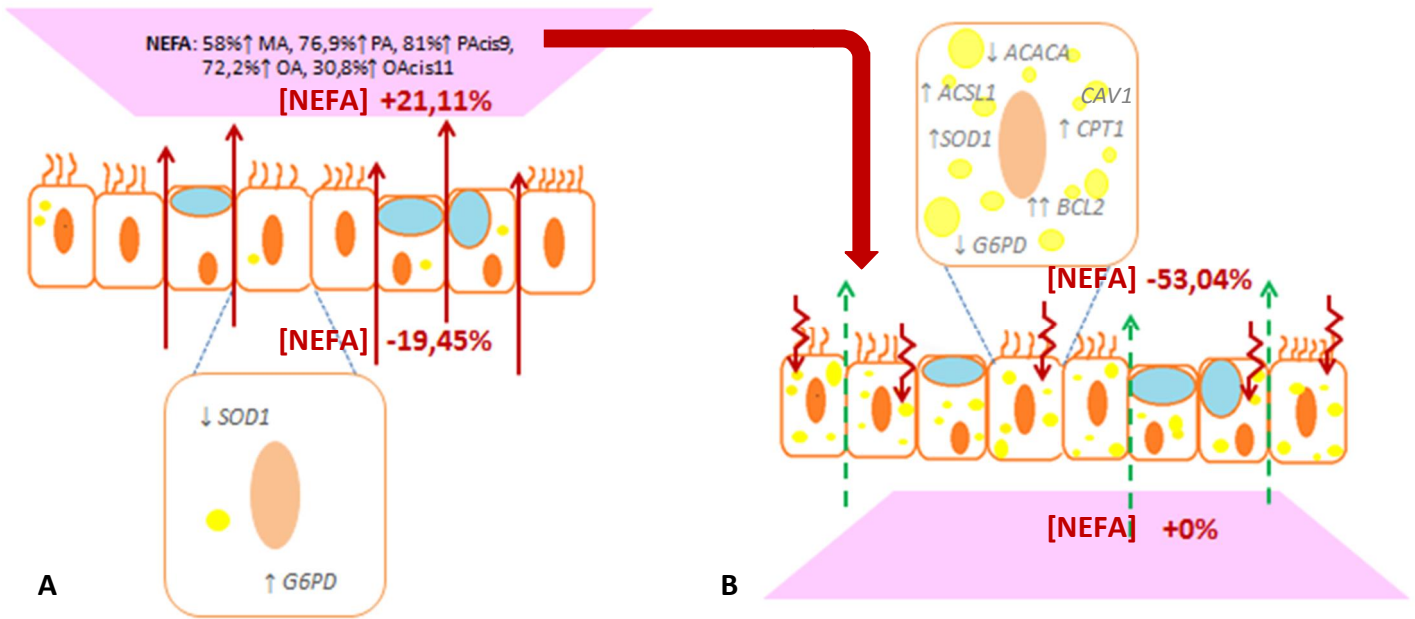


Figure 8



A

B

= ciliated epithelial cell;
 = secretory epithelial cell;
 = lipid droplet;
 = increased basal to apical BOEC-monolayer permeability;
 = intracellular FA-uptake;
 = paracellular FA-transfer;
 = spent medium in apical or basal compartment;

Figure 9